

Electronic supplementary information (ESI)

Catalyst Performance Studies on the Guerbet Reaction in A Continuous Flow Reactor Using Mono- and Bi-metallic Cu-Ni Porous Metal Oxides

Xiao-ying Xi ¹, Zhuo-hua Sun ², Hua-tang Cao ³, Yu-tao Pei ³, Gert H. ten Brink ⁴, Peter J. Deuss ¹, Katalin Barta ^{2,5} and Hero J. Heeres ^{1,*}

¹ Green Chemical Reaction Engineering, Engineering and Technology Institute Groningen, University of Groningen, Nijenborgh 4, 9747 AG Groningen, The Netherlands; x.xi@rug.nl (X.X.); p.j.deuss@rug.nl (P.J.D.)

² Stratingh Institute for Chemistry, University of Groningen, Nijenborgh 4, 9747 AG Groningen, The Netherlands; sunzhuohua@yahoo.com (Z.S.); k.barta@rug.nl (K.B.)

³ Department of Advanced Production Engineering, Engineering and Technology Institute Groningen, Faculty of Science and Engineering, University of Groningen, Nijenborgh 4, 9747AG, The Netherlands; huatang.cao@manchester.ac.uk (H.C.); y.pei@rug.nl (Y.P.)

⁴ Zernike Institute for Advanced Materials, University of Groningen, Nijenborgh 4, 9747 AG, Groningen, the Netherlands; g.h.ten.brink@rug.nl

⁵ Department of Chemistry, Organic and Bioorganic Chemistry, University of Graz, Heinrichstrasse 28/II, 8010 Graz, Austria

* Correspondence: h.j.heeres@rug.nl

Table S1. Chemical composition and textural properties of PMO catalysts.

Catalyst	Theoretical Composition ^a	Experimental Composition ^b	S_{BET}^c , $\text{m}^2 \text{g}^{-1}$	V_{sgp}^d , $\text{cm}^3 \text{g}^{-1}$	D_{BJH}^e , \AA
Cu-PMO	$\text{Cu}_{0.6}\text{Mg}_{2.4}\text{Al}_{1.0}$	$\text{Cu}_{0.6}\text{Mg}_{2.4}\text{Al}_{1.0}$	197.7	0.96	212
Ni-PMO	$\text{Ni}_{0.6}\text{Mg}_{2.4}\text{Al}_{1.0}$	$\text{Ni}_{0.6}\text{Mg}_{2.1}\text{Al}_{1.0}$	239.2	0.74	176
CuNi-PMO	$\text{Cu}_{0.3}\text{Ni}_{0.3}\text{Mg}_{2.4}\text{Al}_{1.0}$	$\text{Cu}_{0.3}\text{Ni}_{0.3}\text{Mg}_{2.3}\text{Al}_{1.0}$	255.7	1.06	173

^a based on quantities of metal ions used during coprecipitation process; ^b Determined by ICP-OES analysis; ^c Specific surface area by BET method; ^d Single point pore volume; ^e Pore diameter by BJH method.

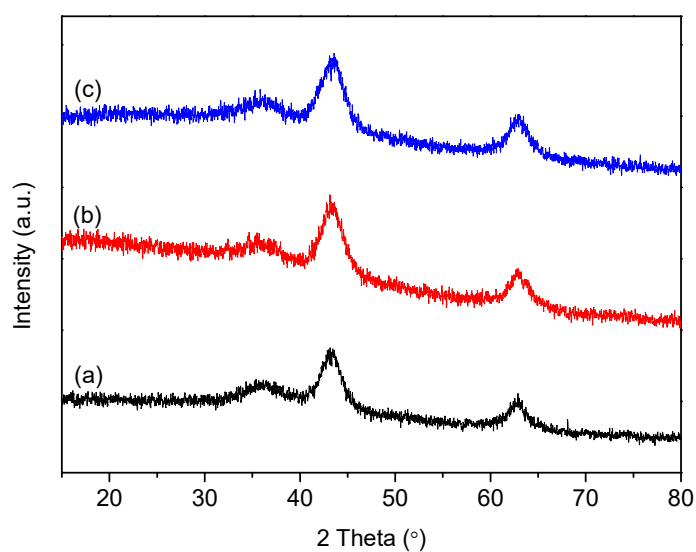


Figure S1. XRD patterns of fresh Cu-PMO (a), Ni-PMO (b) and CuNi-PMO (c) catalyst.

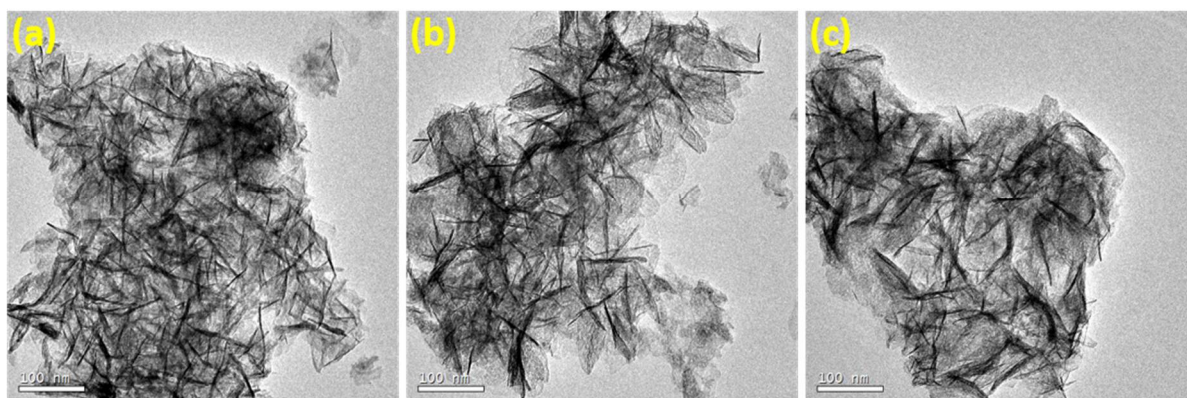


Figure S2. Representative TEM images of fresh Cu-PMO (a), Ni-PMO (b) and CuNi-PMO (c) catalyst.

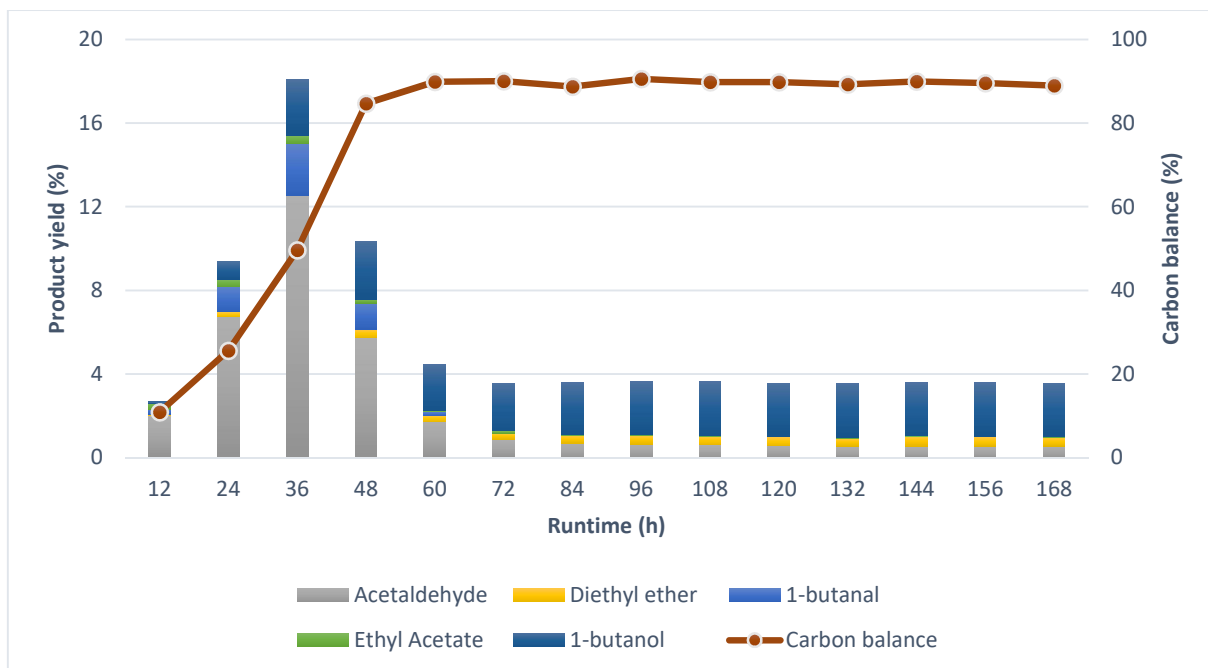


Figure S3. Product yield and carbon balances versus runtime for the CuNi-PMO catalyst. Reaction conditions: 320 °C, 0.1 MPa, LHSV=15 mL g⁻¹ h⁻¹.

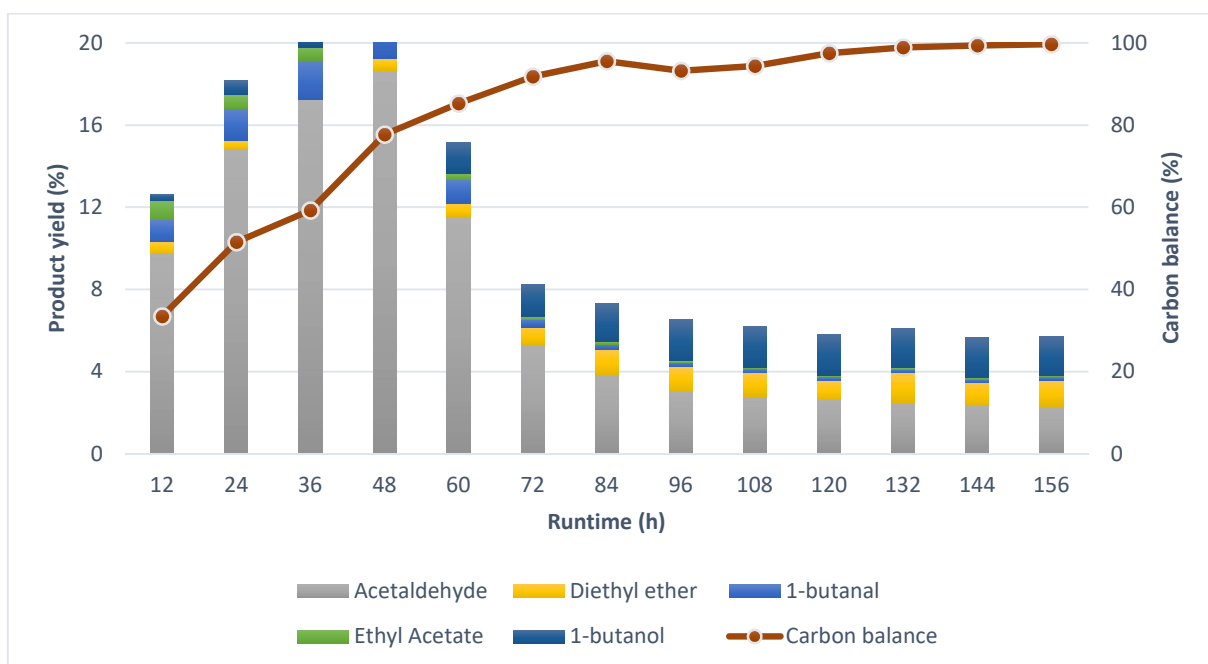


Figure S4. Product yield and carbon balance versus runtime for the Cu-PMO catalyst. Reaction conditions: 320 °C, 0.1 MPa, LHSV=15 mL g⁻¹ h⁻¹.

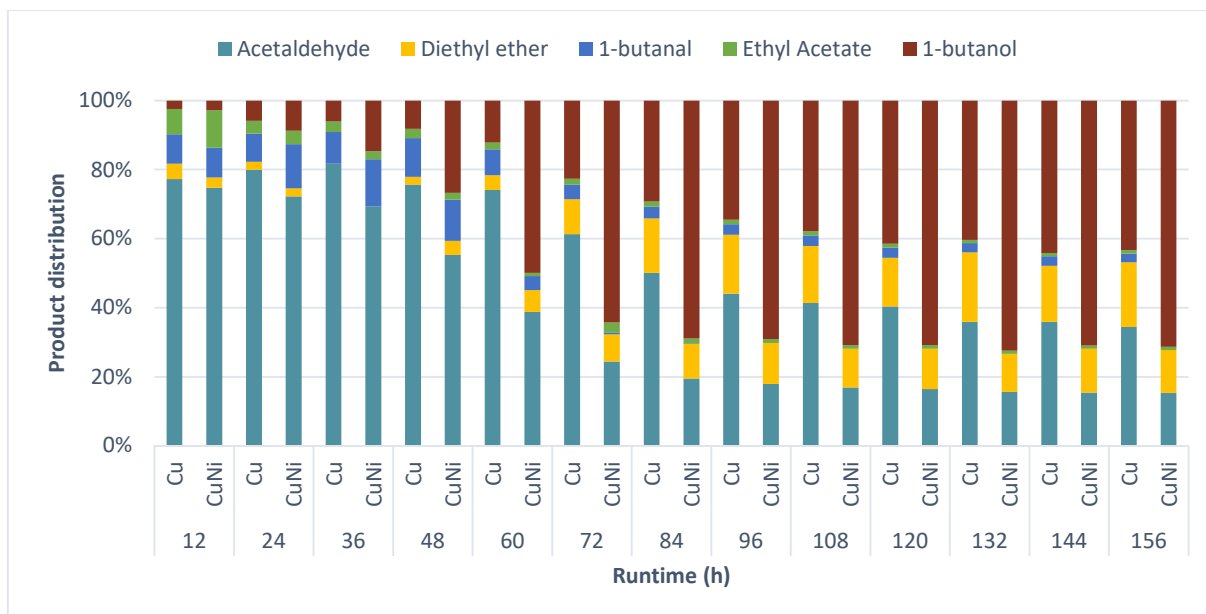


Figure S5. Comparison of product distribution versus runtime for the Cu-PMO and CuNi-PMO catalyst. Reaction conditions: 320 °C, 0.1 MPa, LHSV=15 mL g⁻¹ h⁻¹.

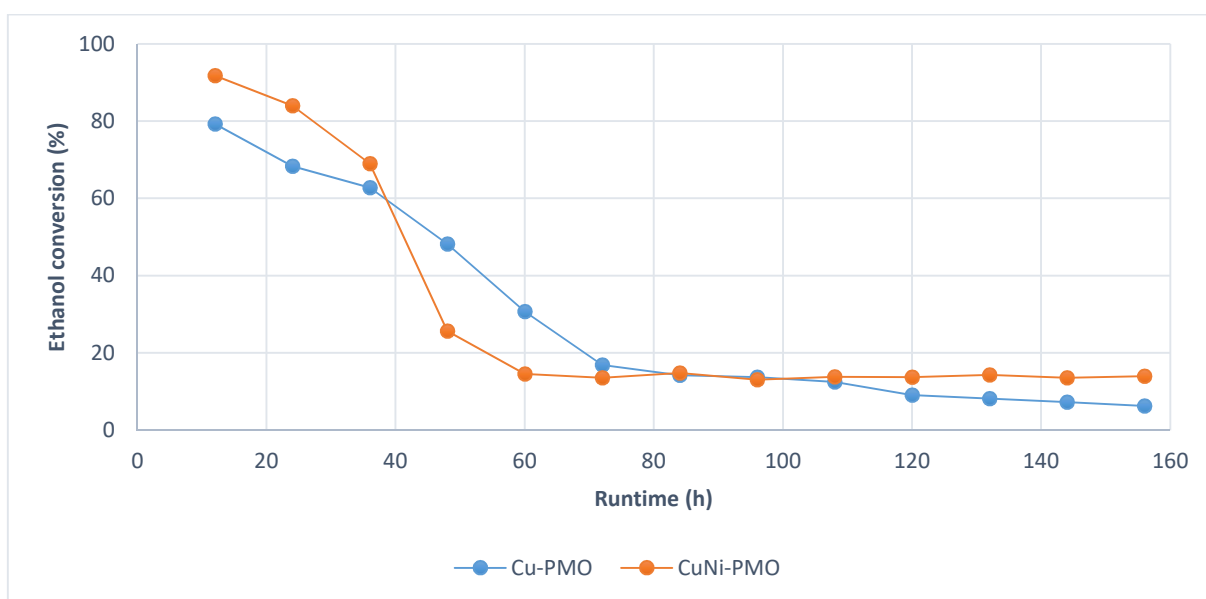


Figure S6. Comparison of ethanol conversion versus runtime for the Cu-PMO and CuNi-PMO catalyst. Reaction conditions: 320 °C, 0.1 MPa, LHSV=15 mL g⁻¹ h⁻¹.

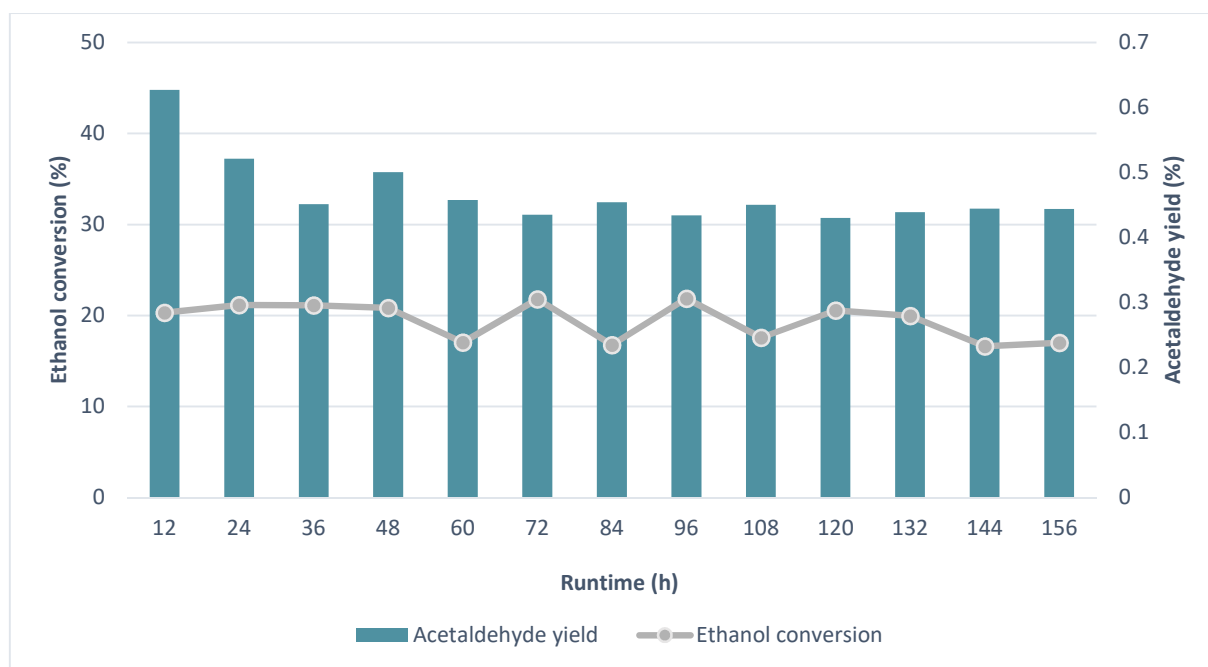


Figure S7. Ethanol conversion and acetaldehyde yield versus runtime for the Ni-PMO catalyst. Reaction conditions: 320 °C, 0.1 MPa, LHSV=15 mL g⁻¹ h⁻¹.

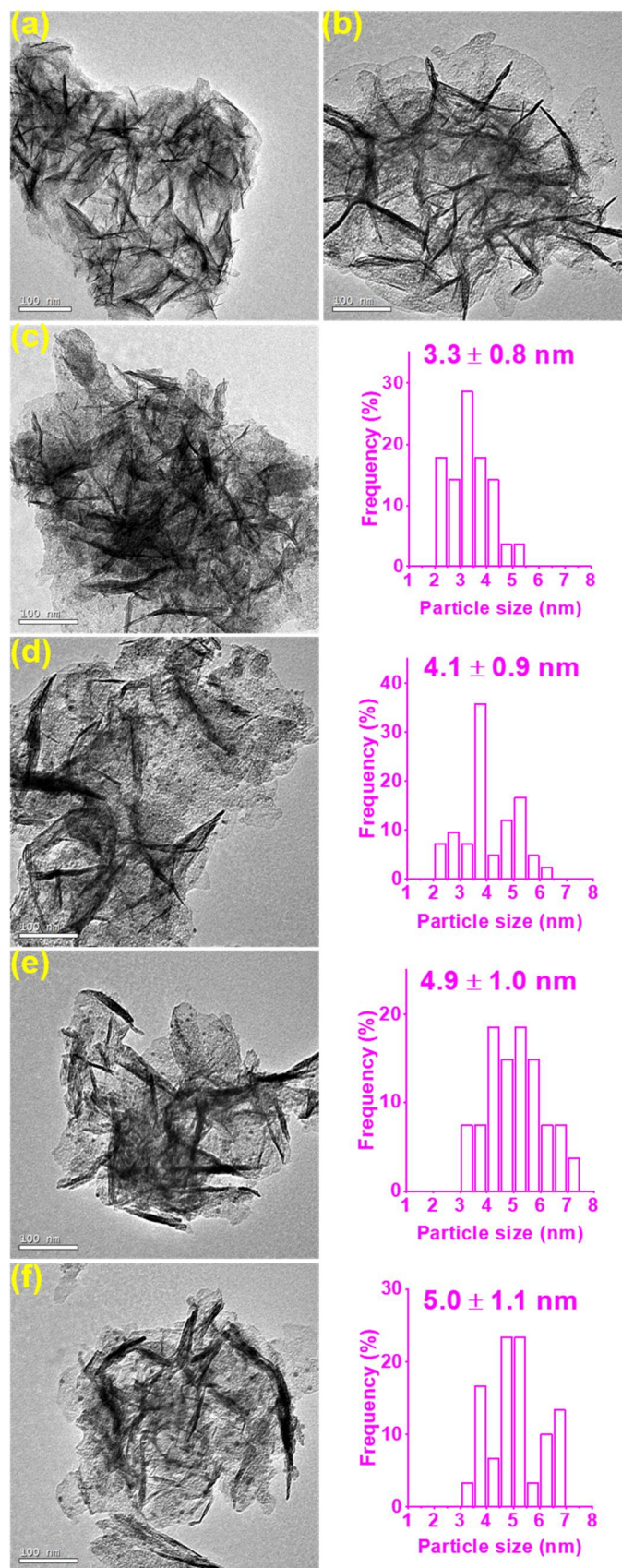


Figure S8. TEM images (scale bar = 100 nm) of fresh and spent CuNi-PMO catalyst after running for different time. Fresh one (a), 24 h (b), 48 h (c), 96 h (d), 123 h (e) and 168 h (f).

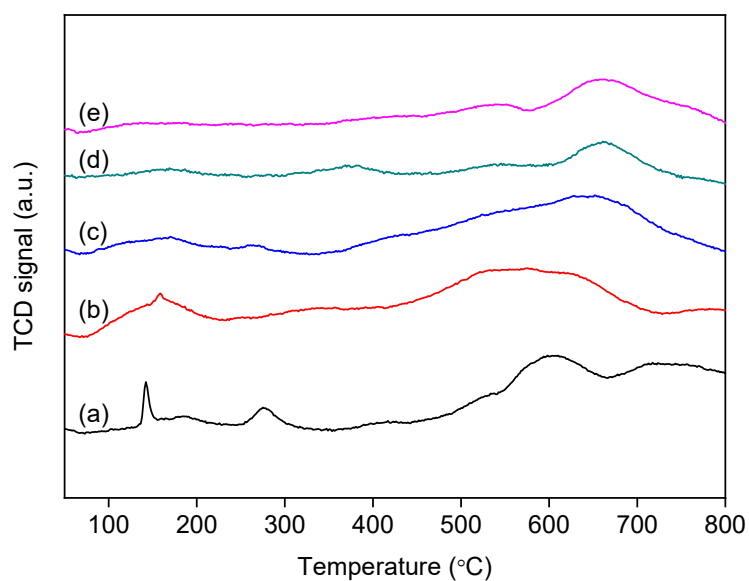


Figure S9. H₂-TPR profiles of spent CuNi-PMO catalyst after running for different time. 24 h (a), 48 h (b), 96 h (c), 123 h (d) and 168 h (e).

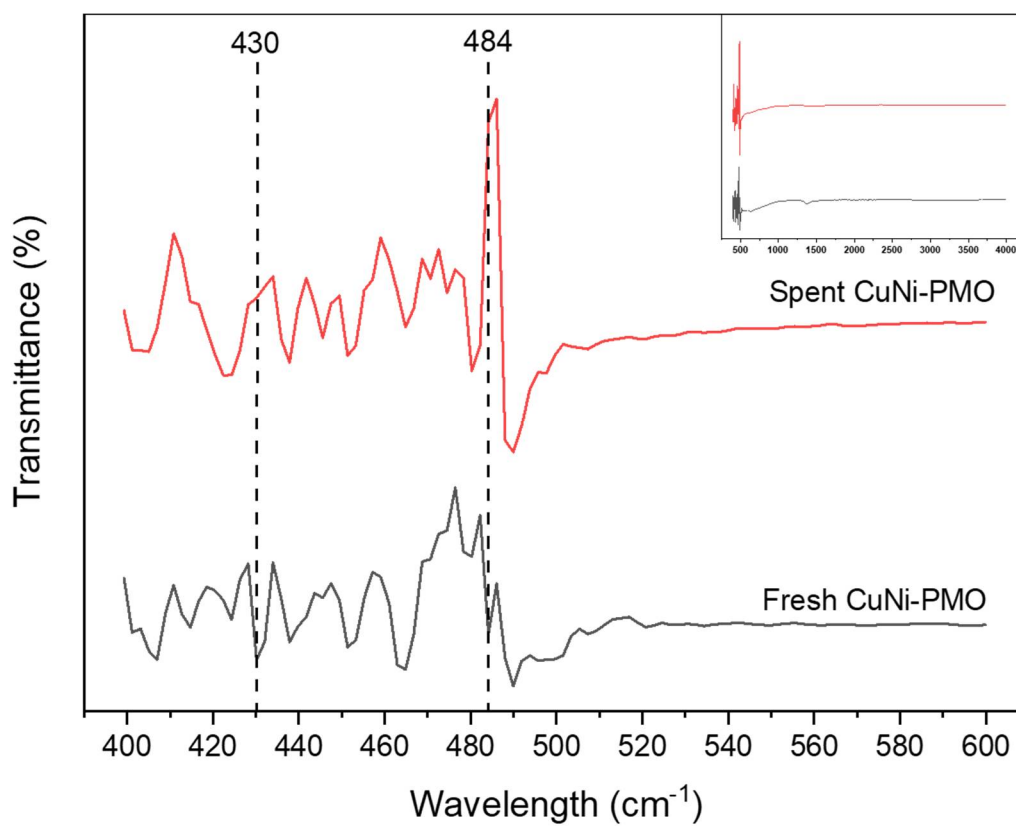


Figure S10. FTIR spectra of fresh and spent CuNi-PMO catalyst obtained after long time (168 h) reaction.

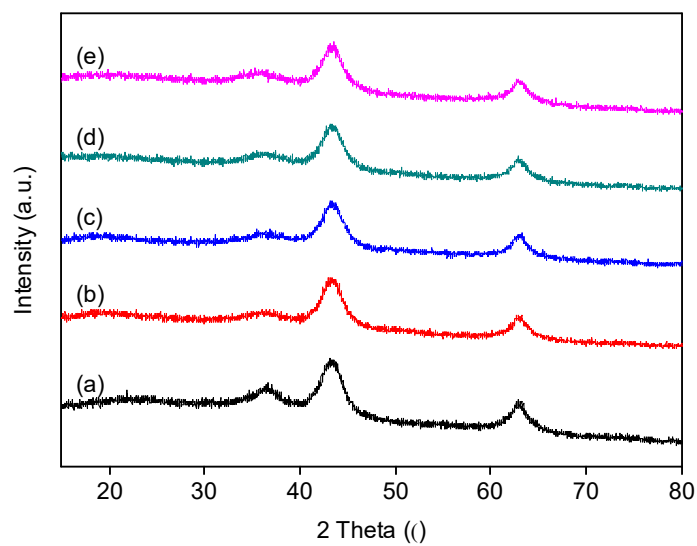


Figure S11. XRD patterns of spent CuNi-PMO catalyst after running for different time. 24 h (a), 48 h (b), 96 h (c), 123 h (d) and 168 h (e).

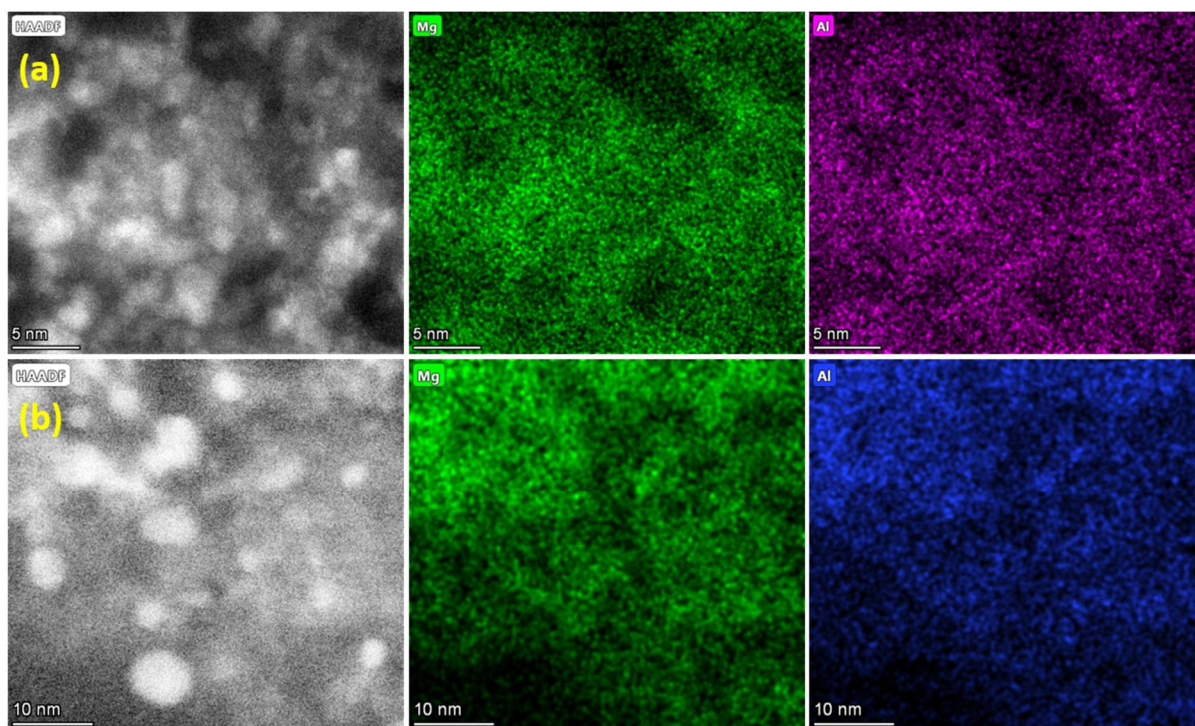


Figure S12. The dark field TEM images and corresponding EDS mapping of Mg and Al for fresh CuNi-PMO (a) and spent CuNi-PMO (b) obtained after 168 h.

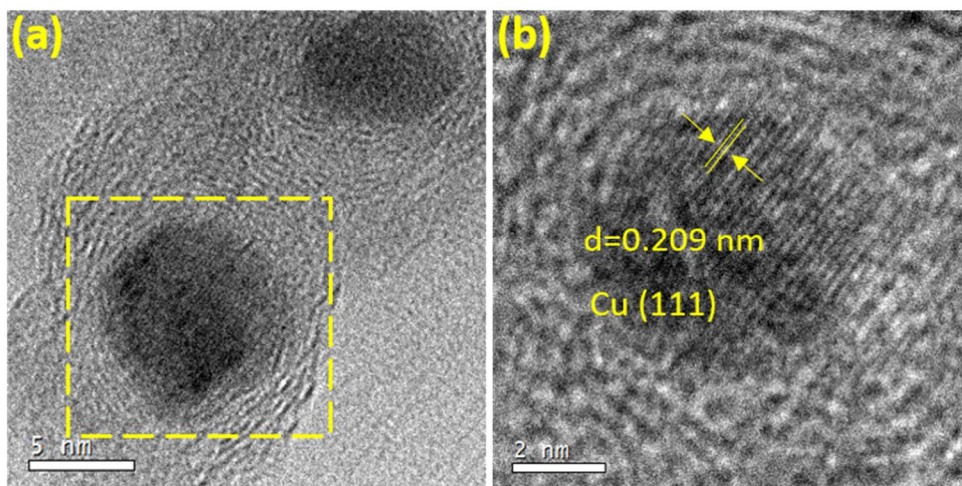


Figure S13. HRTEM images of spent CuNi-PMO catalyst obtained after 168 h. (b) is the close-view of the marked area in (a).

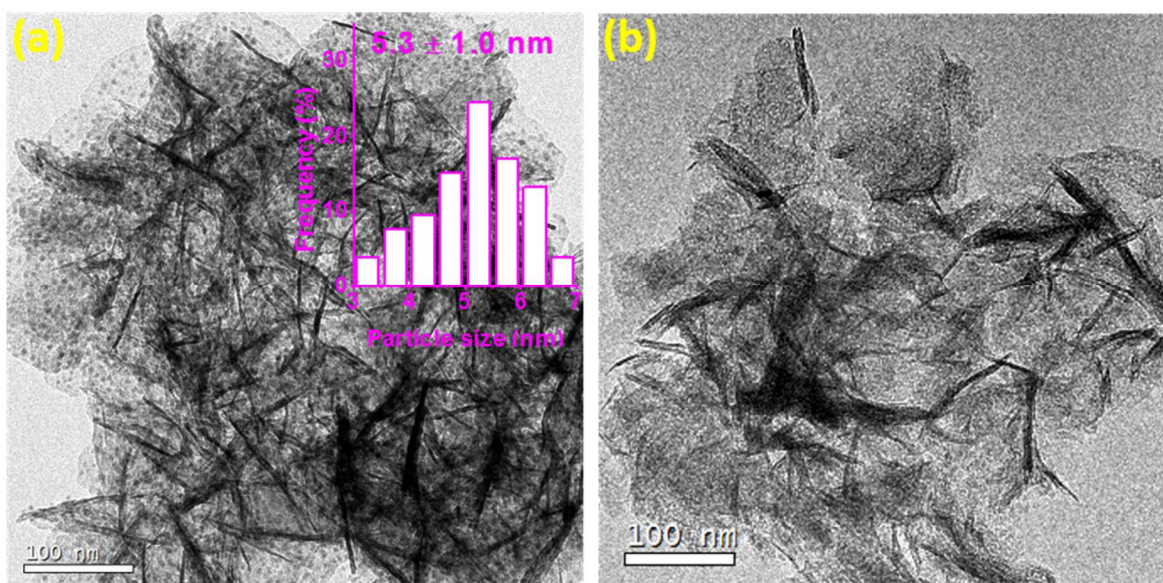


Figure S14. TEM images of spent Cu-PMO (a) and Ni-PMO (b) catalyst obtained after long time reaction.

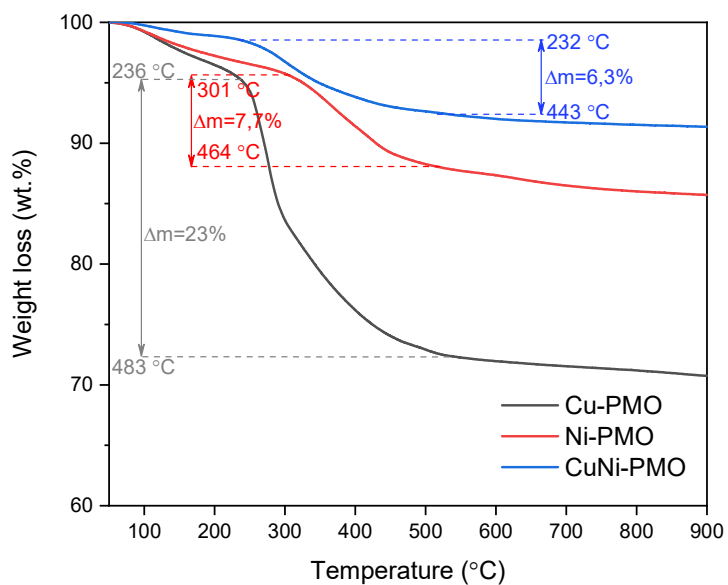


Figure S15. TG curves for the PMO catalysts after extended runtimes (~160 h).

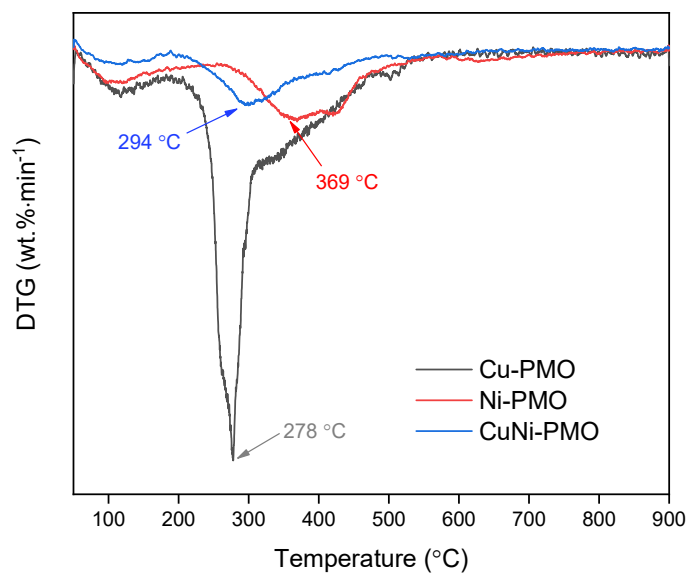


Figure S16. DTG curves for the PMO catalysts after extended runtimes (~160 h).

Table S2. The elemental composition of the CuNi-PMO catalysts before and after reaction (168 h).

Sample	Cu (wt%)	Ni (wt%)	Mg (wt%)	Al (wt%)
Fresh CuNi-PMO	7.4	6.6	21.2	10.4
Spent CuNi-PMO	7.3	6.7	21.2	10.5

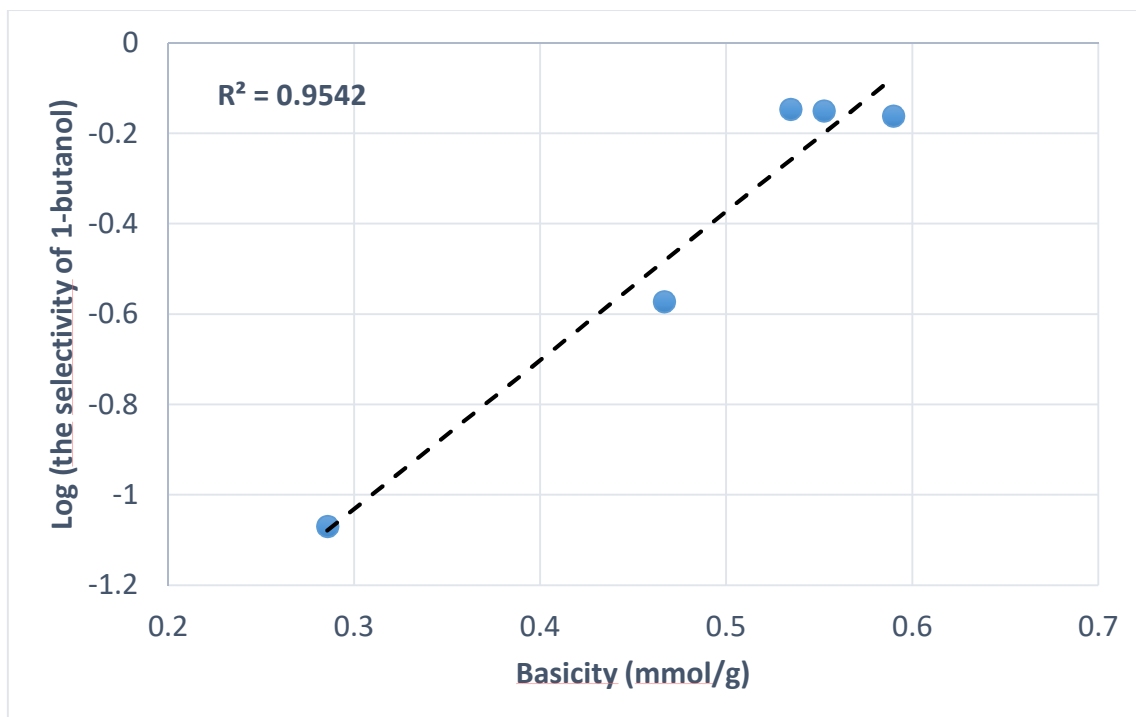


Figure S17. Relationship between basicity and the 1-butanol selectivity for the CuNi-PMO catalyst

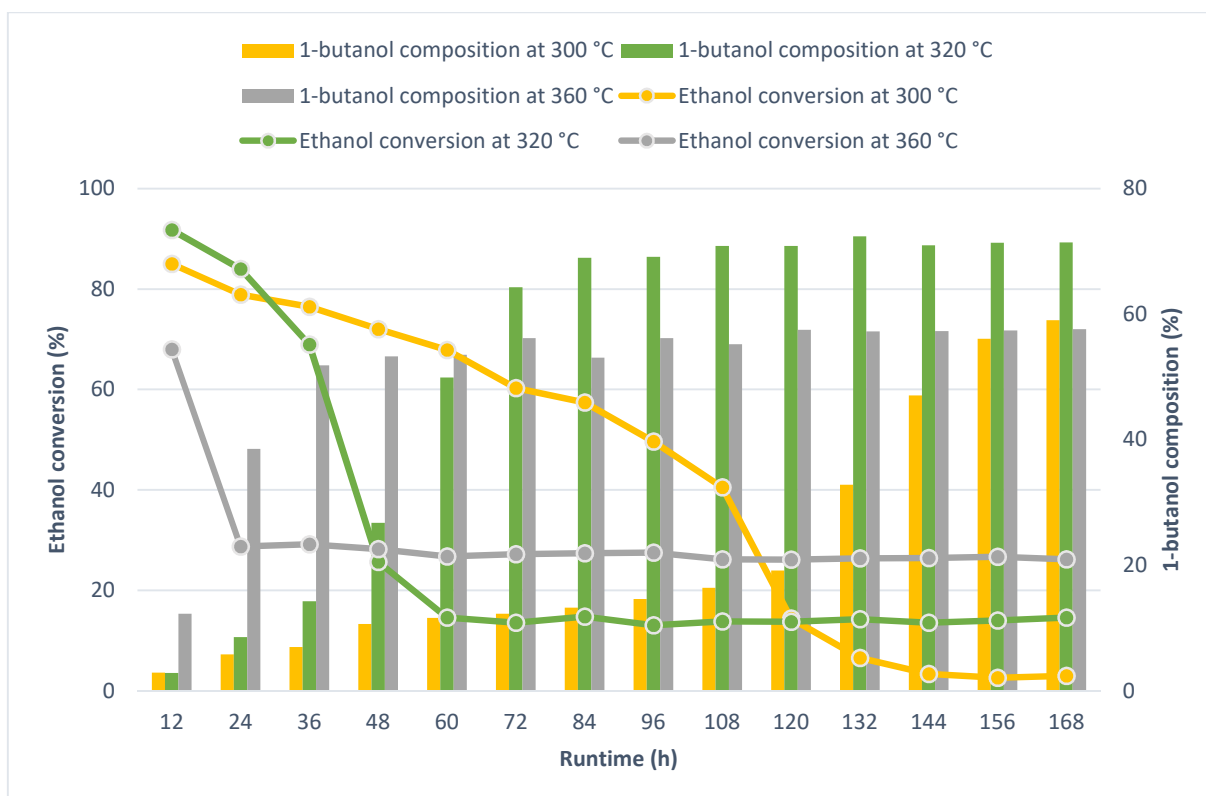


Figure S18. The variation of ethanol conversion and 1-butanol composition with runtime at different temperatures over CuNi-PMO catalyst. Reaction conditions: 0.1 MPa, LHSV = 15 mL g⁻¹ h⁻¹.

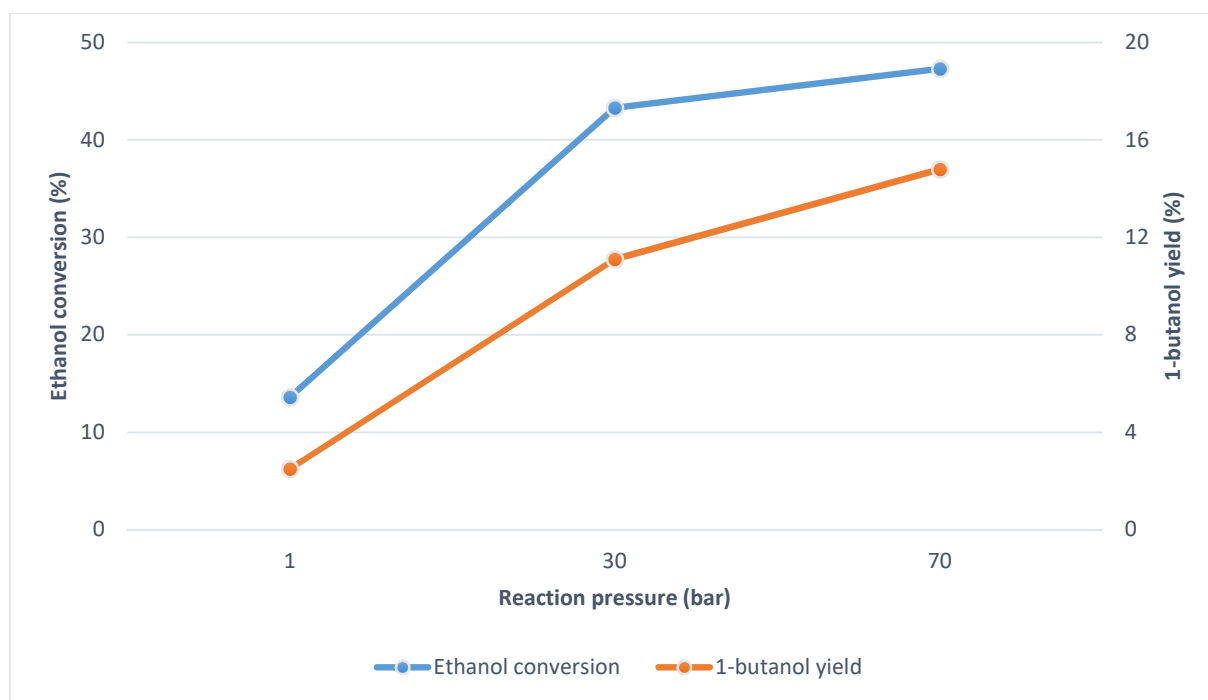


Figure S19. Influence of reaction pressure on ethanol conversion and 1-butanol yield over CuNi-PMO catalyst. Reaction conditions: 320 °C, LHSV=15 mL g⁻¹ h⁻¹.

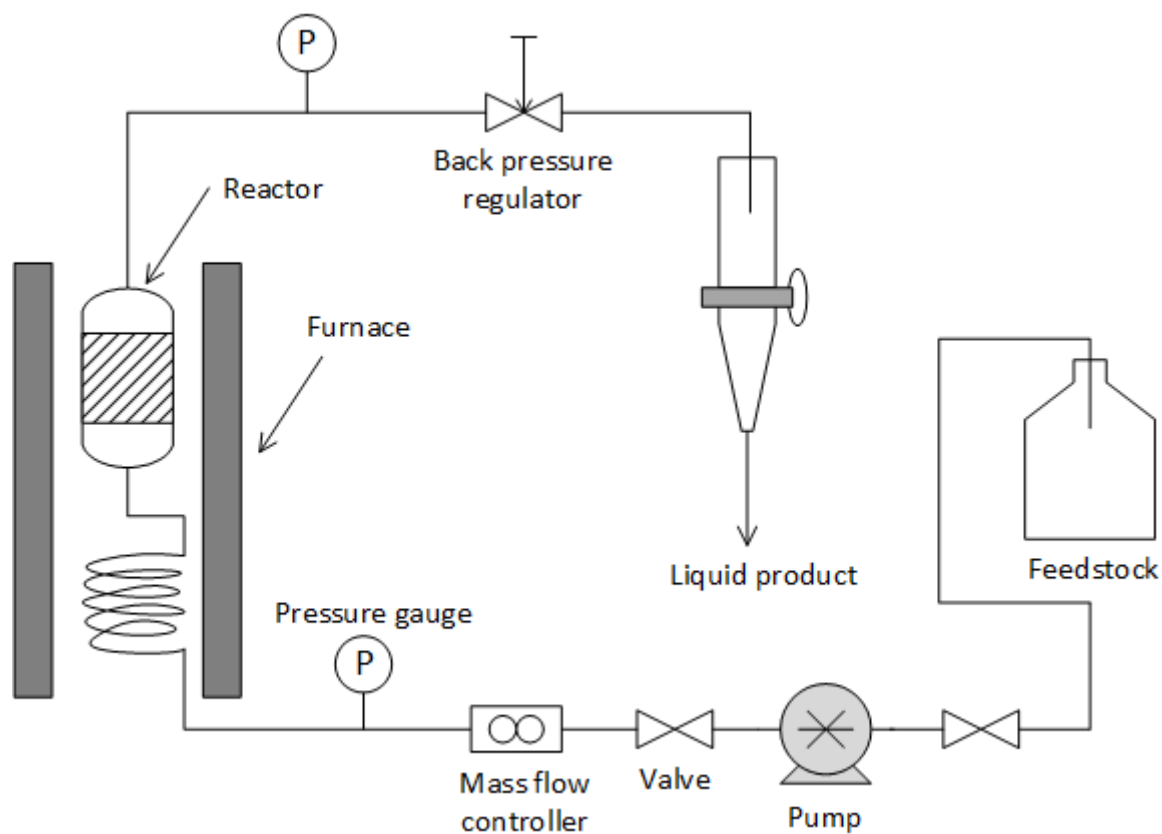


Figure S20. Schematic diagram of the continuous set-up for Guerbet coupling of ethanol.

Table S3. Duplicate experiments showing ethanol conversion and product yield versus runtime for the CuNi-PMO catalyst. Reaction conditions: 260-360 °C, 0.1 MPa, LHSV=15 mL g⁻¹ h⁻¹.

Temperature (°C)	Runtime (h)	Ethanol conversion (%)		Yield (%)									
				Acetaldehyde		Diethyl ether		1-Butanal		Ethyl acetate		1-Butanol	
		Run 1	Run 2	Run 1	Run 2	Run 1	Run 2	Run 1	Run 2	Run 1	Run 2	Run 1	Run 2
260	8	43.3%	44.5%	11.8%	13.7%	3.1%	3.0%	0.6%	0.7%	0.8%	0.9%	1.4%	1.5%
260	16	46.2%	43.6%	15.7%	14.5%	4.8%	4.2%	1.1%	0.9%	0.8%	0.8%	1.8%	1.7%
260	24	46.8%	45.5%	15.4%	13.8%	3.6%	3.8%	1.5%	1.3%	0.5%	0.7%	2.9%	3.0%
280	32	57.8%	56.7%	13.9%	13.0%	2.9%	2.6%	2.4%	2.9%	0.3%	0.2%	4.0%	3.8%
280	40	59.6%	57.6%	14.0%	13.4%	2.6%	2.7%	3.6%	3.9%	0.2%	0.3%	6.0%	5.8%
280	48	55.5%	59.8%	13.1%	13.9%	4.3%	3.8%	3.9%	3.8%	0.2%	0.2%	6.7%	6.8%
300	56	67.8%	69.0%	11.5%	11.1%	2.2%	2.3%	4.0%	4.5%	0.1%	0.2%	5.4%	5.6%
300	64	69.3%	67.7%	12.0%	11.9%	2.8%	2.3%	4.5%	4.6%	0.1%	0.1%	5.8%	5.5%
300	72	64.0%	68.3%	12.8%	12.4%	2.5%	2.4%	4.3%	3.8%	0.1%	0.1%	5.9%	5.8%
320	80	71.0%	72.4%	11.5%	12.8%	2.0%	1.7%	3.9%	4.4%	0.1%	0.1%	4.4%	4.3%
320	88	51.3%	50.1%	9.2%	9.1%	2.6%	2.5%	2.4%	2.8%	0.1%	0.2%	3.8%	3.8%
320	96	17.8%	18.3%	3.7%	3.6%	3.3%	3.2%	0.5%	0.5%	0.0%	0.1%	2.6%	3.2%
320	104	19.2%	17.6%	1.6%	1.8%	3.1%	3.2%	0.2%	0.1%	0.0%	0.1%	2.4%	2.7%
320	112	14.4%	15.9%	1.4%	1.6%	3.2%	3.2%	0.1%	0.2%	0.0%	0.2%	2.6%	2.8%
320	120	15.0%	16.4%	1.3%	1.4%	3.6%	3.7%	0.1%	0.2%	0.0%	0.1%	2.7%	2.7%
340	128	19.1%	20.1%	1.5%	1.8%	4.1%	4.6%	0.1%	0.1%	0.0%	0.1%	4.3%	4.2%
340	136	20.6%	18.9%	1.6%	1.6%	3.8%	4.0%	0.1%	0.1%	0.0%	0.0%	5.1%	5.5%
340	144	17.6%	18.7%	1.7%	1.4%	4.8%	4.2%	0.1%	0.1%	0.0%	0.0%	5.2%	5.6%
360	152	26.8%	25.3%	2.0%	1.9%	5.8%	5.9%	0.2%	0.2%	0.0%	0.1%	7.2%	7.5%
360	160	25.2%	24.5%	2.3%	2.0%	5.8%	5.6%	0.2%	0.2%	0.1%	0.2%	7.6%	7.4%
360	168	22.8%	23.4%	2.3%	2.3%	6.3%	6.3%	0.2%	0.3%	0.1%	0.1%	7.5%	7.1%